

Fold removal in CT Colonography: A Physics-Based Method

Padmavathi Sundaram^{1,2**}, David S. Paik¹, Eftychios Sifakis³, Christopher F. Beaulieu¹, and Sandy Napel¹

¹ Department of Radiology, Stanford University, Stanford, CA 94305

² Department of Electrical Engineering, Stanford University, Stanford, CA 94305

³ Department of Computer Science, Stanford University, Stanford, CA 94305

Abstract. Computed Tomographic Colonography (CTC) produces 2-d and 3-d images of the colon using computed tomography (CT). The main goal of CTC is to detect small lumps on the colon surface called polyps, which are known to be precursors to colon cancer. Radiologists are therefore interested in exploring the inner surface of the colon to detect polyps. Polyps may be detected by visual inspection of colon CT images and also by using computer-aided detection. The colon surface is abundant with folds that occlude polyps during visual inspection and also contribute to false positives in computer-aided polyp detection. Removal of folds should therefore improve visualization and could also improve polyp detection sensitivity. In this paper, we present a physics-based method to unfold the colon surface. The output of our algorithm is a surface in 3-d, with the folds flattened out, leaving only polyps behind. Preliminary tests of our method in mathematical phantoms and actual patient data show reductions in fold height and curvature ranging from 54.4% to 70.3%, and 36.3% to 86.1% respectively. Polyp size and curvature were reduced by only 0 to 16%, and 0 to 20%, respectively. Our method, thus, demonstrates potential for improving both visual and computer-aided detection of colonic polyps from CTC examinations.

1 Introduction

Colon cancer is the second leading cause of cancer deaths in the United States, with over 100,000 new cases and over 55,000 deaths expected in 2005[1]. Traditionally, the colon surface is examined using colonoscopy, which involves the use of a lit, flexible fiberoptic or video endoscope to detect small lumps on the colon surface called polyps. Polyps are known to be precursors to colon cancer[2, 3].

Computed Tomographic Colonography (CTC), under development as a less invasive alternative to colonoscopy, produces 2-d and 3-d images of the colon using CT[4]. In CTC, radiologists examine hundreds of 2-d images and/or 3-d computer graphics renditions of the colonic surface to detect polyps.

Three dimensional surface images rendered from an internal perspective (“virtual fly-through” or “virtual colonoscopy”) appear similar to those produced

** email: padma@stanford.edu

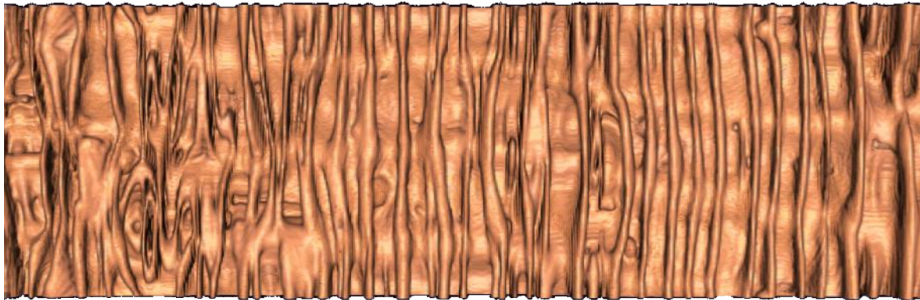


Fig. 1. Virtual dissection view of the colon. The colon surface is mathematically cut and flattened, enabling comprehensive inspection. Note the abundance of vertically-oriented haustral folds.

by conventional colonoscopy. However, navigation through a tortuous, complex structure like the colon is challenging and, frequently, portions of the colonic surface may be missed, leading to incomplete examinations. Cylindrical and planar map projections have been proposed to increase the viewable surface during fly-through, but the presentation format is unfamiliar and the physician may still not have a complete view[5, 6].

An alternative approach is to mathematically cut the tubular colon surface and lay it out flat for a comprehensive inspection, as shown in figure 1. In order to do this, planar cross-sections are computed orthogonal to the central path of the colon. The surface is then unfolded using a polar-to-Cartesian coordinate transformation[7, 8]. However, in high curvature portions of the path, the surface may either be under- or over-sampled, causing surface features to either appear multiple times or be missed completely. Various methods have been proposed to correct for problems caused by non-uniform sampling[9–11]. But, no matter which method is used, the output is abundant in haustral folds, which occlude polyps and make it difficult for both, visual and computer-aided detection of polyps.

In this paper, we present a method to straighten the colon and flatten it. Our output is a 3-d surface that can be displayed in a single image. In order to flatten the colonic surface, we simulate stretching of the surface using a quasistatic finite element model. Since the folds are highly directional, stretching the surface in a direction normal to the direction of the folds, results in attenuating the folds, leaving only largely undistorted polyps. The key contribution of our work is that, unlike the other approaches, the flattened view generated by our algorithm does not contain folds. This physics-based manipulation of the colonic surface to attenuate folds, while preserving polyps, is a novel paradigm, and has the potential to change the way colon CT data is visualized and interpreted.

The rest of this paper is organized as follows. Section 2 has 3 parts. We begin by describing the finite element model in section 2.1. In section 2.2, we

describe the setup of our simulation system. Section 2.3 describes the quasistatic assumption made in the simulation. This implies that inertial effects were neglected, ie. the system simulated had zero acceleration, resulting in a zero mass effect. This assumption is important to ensure a spatially invariant response to the stretching forces. In section 3, we describe experiments that we performed in simulated and actual patient data and report results quantifying the behavior of our method. Section 4 discusses the limitations of this work, possible future research, and conclusions.

2 Method

In order to simulate stretching of the colon surface, a physics-based model must first be selected. We chose between mass spring models and finite element models (FEM). In section 2.1, we explain our model choice.

2.1 Choice of a physics-based model

We start by creating a triangulated isosurface at the air-mucosa boundary from the CT image data. Our algorithm is independent of the triangulation, so any desired meshing scheme may be used. The meshes used in this work were created using the scheme described in [12], but applied to triangle meshes.

In order to physically manipulate the mesh, a physics-based model must be imparted to it. We chose between mass spring models and FEMs, which have been both used for deformable modeling in graphics[13, 14]. Mass spring models are easy to formulate but setting the spring constants correctly can be extremely difficult. Also, the global mechanical properties are dependent on mesh topology, which may, in turn, generate undesired anisotropy. Since our algorithm requires imparting global material properties to the surface, we chose the finite element model over the mass spring system.

The main difference between the mass spring system and the FEM is the manner in which the nodal forces are calculated. In the FEM, we write out constitutive equations for the material describing the relationship between the strain (deformation measure) and the stress (internal forces). The forces at the mesh nodes are then computed using a discretized version of the constitutive equations.

In selecting a constitutive model, we were looking for a specific qualitative material behavior. The exact quantitative model was less important. In order to flatten folds but not polyps, it is desirable for the material to be soft under very small strains, but become very stiff under large strain conditions. We used a neo-hookean elasticity model for the surface being stretched[15]. A nonlinear elasticity model was preferred over a linear elasticity one since we are dealing with large deformations.

The two important material properties that needed to be set were Young's modulus and Poisson's ratio. Young's modulus is the ratio of longitudinal stress to longitudinal strain (with the force applied in the longitudinal direction), and

represents the stiffness of the material and was set to a high value (50,000). Basically, the material was stiff enough to allow the fold to flatten while the polyps remained undistorted. Poisson’s ratio is the ratio of the axial strain to the longitudinal strain in response to a longitudinal stretching force which, in all common materials, causes them to become narrower in cross-section while being stretched. We wanted to minimize this contraction, and so we set the Poisson’s ratio to a very small positive number (1×10^{-10}).

These material properties were selected so as to result in a desired behavior when the stretching forces were applied. It must be emphasized that the goal here was not to create a realistic simulation of the behavior of actual mucosal tissue when stretched. Rather it was to selectively flatten colonic folds while leaving polyps undistorted using a physical system to evolve the surface.

In order to simulate stretching of the surface, (external) forces are applied to the ends. We then need to compute for the positions of the mesh nodes at each time step of the simulation. The new positions are a function of the internal forces, which are computed using the constitutive equations and the surface deformation. In the next section, we describe our simulation system.

2.2 System Description

Our simulation system treats the triangulated colon surface as a particle system[16]. Each node in the mesh is a particle having mass, position, velocity, zero spatial extent and responding to forces.

The motion of a single particle is described by Newton’s second law using

$$\mathbf{f} = m\mathbf{a}.$$

Since $\mathbf{a} = \dot{\mathbf{v}}$ and $\mathbf{v} = \dot{\mathbf{x}}$, this second order equation may be broken down into two first order equations:

$$\begin{aligned}\dot{\mathbf{x}} &= \mathbf{v} \\ \dot{\mathbf{v}} &= \frac{\mathbf{f}}{m},\end{aligned}$$

where \mathbf{x} , \mathbf{v} and \mathbf{f} are 3-vectors and denote the position, velocity and the force at a single node in the mesh.

To describe the evolution of the complete deformable surface, we concatenate the positions, velocities and the aggregate forces of all the nodes in the mesh into single n -vectors, where n is the number of nodes in the mesh. Thus we get,

$$\begin{aligned}\dot{\mathbf{x}} &= \mathbf{v} \\ \dot{\mathbf{v}} &= M^{-1}\mathbf{f}(t, \mathbf{x}, \mathbf{v})\end{aligned}$$

where M represents the diagonal mass matrix.

The force \mathbf{f} at each node is the sum of the internal and external forces acting on that node. The external forces are the user-supplied time varying input to the system. In our case, the external forces are the pulling forces applied to the

ends of the surface being stretched. Internal forces represent the resistance of the material to the external forces applied.

So far, we have discussed the simulation system and the computation of internal forces as a function of deformation and the material constitutive model. Ideally, the response to the stretching forces should be spatially invariant. Otherwise, polyps located at different spatial locations will be distorted (stretched) by different amounts. In order to achieve this, we assume that the mesh is zero mass, thus giving rise to zero acceleration. This assumption is called the quasistatic assumption, since it neglects inertial effects and solves for static equilibrium at each time step. We describe this in more detail in the next section.

2.3 Quasistatic assumption

In order to preserve polyps while flattening folds, it is essential that the response to the stretching forces be spatially invariant. Otherwise, structures closer to the edges being pulled will be more distorted than those farther away. In order to achieve this, we neglect inertial effects. This implies that the system has zero acceleration and zero mass, giving,

$$\mathbf{f}(t, \mathbf{x}, \mathbf{v}) = \mathbf{0}. \quad (1)$$

The quasistatic assumption[17] satisfies equation 1 by enforcing force equilibrium at every time step, implying

$$\mathbf{f}(\mathbf{x}_{k+1}) = \mathbf{f}(\mathbf{x}_k + \Delta\mathbf{x}_k) = \mathbf{0}.$$

Therefore at every time step, a linear system must be solved; for this we used the Newton-Raphson solver,

$$\mathbf{f}(\mathbf{x}_k + \Delta\mathbf{x}_k) \approx \mathbf{f}(\mathbf{x}_k) + \Delta\mathbf{x}_k \left. \frac{\partial \mathbf{f}}{\partial \mathbf{x}} \right|_{\mathbf{x}_k} = \mathbf{0}.$$

We then compute the new nodal positions $\mathbf{x}_{k+1} = \mathbf{x}_k + \Delta\mathbf{x}_k$, by computing $\Delta\mathbf{x}_k$ from,

$$-\Delta\mathbf{x}_k \left. \frac{\partial \mathbf{f}}{\partial \mathbf{x}} \right|_{\mathbf{x}_k} = \mathbf{f}(\mathbf{x}_k).$$

Note that at every time step, we need to invert the global stiffness matrix, $\frac{\partial \mathbf{f}}{\partial \mathbf{x}}$, which is constructed from the contributions of the element stiffness matrices that account for contributions from individual triangles.

To tie the stiffness matrix $\frac{\partial \mathbf{f}}{\partial \mathbf{x}}$, to the constitutive model of the material, note that the constitutive model, which typically relates stress to strain, can also be expressed as a relationship between force and strain energy. So,

$$\mathbf{f} = -\frac{\partial \psi}{\partial \mathbf{x}}$$

where ψ denotes the strain energy.

To summarize, we have described our simulation framework and discussed the physics-based model used. In the next section we present results quantifying the behavior of our method. We also present an example illustrating the importance of using the quasistatic assumption.

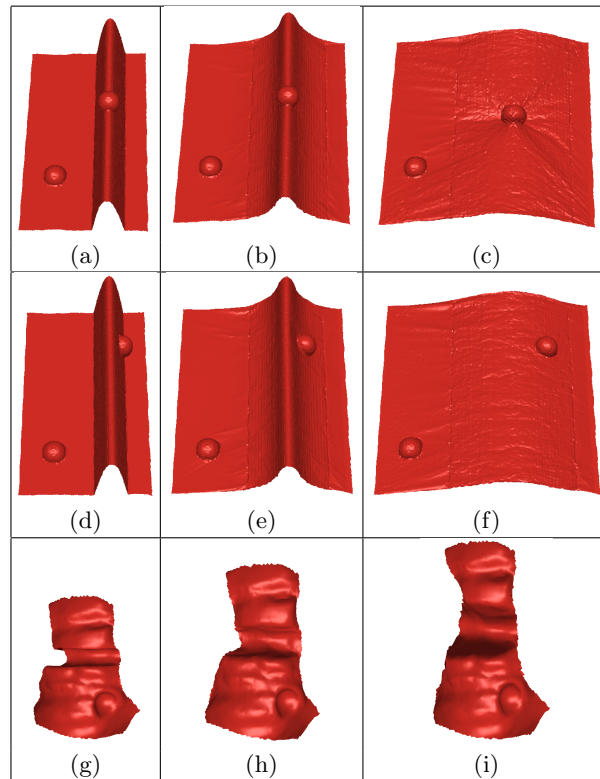


Fig. 2. Results from phantom and actual patient experiments: Each row shows steps in the deformation of a phantom or actual patient data. Figures (a), (b) and (c) show a phantom with a polyp on a flat portion in addition to one on top of a fold, while figures (d), (e) and (f) show a polyp on a flat portion, as well as one on the side of the fold. Figures (g), (h) and (i) show a subvolume of actual patient data being stretched. In all cases, folds were attenuated and relatively undistorted polyps remained.

3 Results

3.1 Results from phantom data

We created mathematical phantoms using MATLAB 7.0.1, with folds and polyps modeled as half sine functions and hemispheres, respectively. Figures 2(a) and

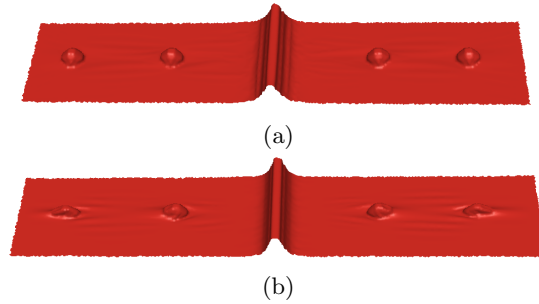


Fig. 3. Illustration of what can go wrong if quasistatic assumption is not made. Comparing single time points in the simulated stretching of a phantom with polyps and folds, with inertial effects neglected in (a), but not in (b). In (b), polyps at different spatial locations were distorted by different amounts. This is undesirable.

2(d) show two of the phantoms we created, illustrating folds, polyps on flat regions and polyps on folds. We measured the curvature and size of polyps (diameters) and folds (height) before and after simulated stretching.

For the phantom in figure 2(a), the height and curvature of the fold were reduced by 70% and 86.1%, respectively. The polyp on top of the fold was distorted in the stretch direction causing an increase in its maximum width by 16%, and a decrease of 20.2% in its maximum curvature. The size and the curvature of the polyp on the surface remained unchanged.

The phantom in figure 2(d) has a polyp on the surface and on the side of the fold. The height and curvature of the fold were reduced by 70.3% and 73.5%, respectively. The sizes and curvatures of both polyps remained unchanged.

Finally, figure 3 illustrates the importance of the quasistatic assumption. If inertial effects are not neglected, polyps at different spatial locations will be distorted by different amounts, as shown in the figure 3(b).

3.2 Results from patient data

Figure 2(g) shows stretching of a subvolume of actual patient data, acquired under our IRB during a research CTC scan at our institution, containing a 6.9 mm polyp. The height and curvature of the fold were attenuated by 54.4% and 36.3%, respectively. The polyp was distorted in the stretch direction causing an increase of 10% in its maximum width, and a decrease of 10% in its maximum curvature.

4 Discussion

There are several aspects of the current algorithm that need further work. The stopping criterion for the simulation is currently not automated. We are working

on incorporating a strain-based stop criterion into the algorithm. Also, all the examples shown have folds that extended along the entire width of the surface. Individual haustral folds typically subtend about $\frac{1}{3}$ of the luminal circumference. We are working on modifying our algorithm to handle these cases.

In conclusion, we presented a method to straighten and flatten the colonic surface as acquired using cross-sectional imaging using a physics-based approach employing a quasistatic finite element model. The output of the algorithm is a 3-d surface with the surface folds flattened and with polyps relatively undistorted. Removal of folds not only reduces clutter in visualization but can also reduce false positives in computer-aided polyp detection. The results of this preliminary work give a proof of concept; further studies on real patient data sets are required.

References

1. Jemal, A., Murray, T., Ward, E., Samuels, A., Tiwari, R.C., Ghafoor, A., Feuer, E.J., Thun, M.J.: Cancer statistics, 2005. *CA Cancer Journal for Clinicians* **55** (2005) 10–30
2. Muto, T., Bussey, H.J., Morson, B.C.: The evolution of cancer of the colon and rectum. *Cancer* **36** (1975) 2251–2270
3. Eide, T.J.: Natural history of adenomas. *World Journal of Surgery* **15** (1991) 3–6
4. Vining, D.: Virtual endoscopy: Is it reality. *Radiology* **200** (1996) 30–31
5. Beaulieu, C.F., Jeffrey, R.B., Karadi, C., Paik, D.S., Napel, S.: Display modes for CT colonography. Part II. Blinded Comparison of axial CT and virtual endoscopic and panoramic endoscopic volume-rendered studies. *Radiology* **212** (1999) 203–212
6. Paik, D., Beaulieu, C., Jeffrey, R., Karadi, C., Napel, S.: Visualization Modes for CT Colonography using Cylindrical and Planar Map Projections. *Journal of Computer Assisted Tomography* **24** (2000) 179–188
7. Wang, G., Vannier, M.W.: GI tract unraveling by spiral CT. *SPIE* **2434** (1995) 307–315
8. Sorantin, E., Balogh, K., Werkgartner, G., Spuller, E., Loncaric, S.: Technique of Virtual Dissection of the Colon based on Spiral CT data. In: *Medical Radiology - Diagnostic Imaging*. Springer Verlag Press (2001)
9. Wang, G., McFarland, E.G., Brown, B.P., Vannier, M.W.: GI Tract Unraveling with Curved Cross Sections. *IEEE Transaction on Medical Imaging* **17** (1998)
10. Bartrolí, A.V., Wegenkittl, R., König, A., Gröller, E.: Nonlinear virtual colon unfolding. In: *Proceedings of IEEE Visualization 2001*. (2001) 411–418
11. Haker, S., Angenent, S., Tannenbaum, A., Kikinis, R.: Non-distorting Flattening Maps and the 3-D Visualization of Colon CT images. *IEEE Transactions on Medical Imaging* **19** (2000) 665–670
12. Molino, N., Bridson, R., Teran, J., Fedkiw, R.: A crystalline, red green strategy for meshing highly deformable objects with tetrahedra. *12th Int. Meshing Roundtable* (2003) 103–114
13. Bridson, R., Marino, S., Fedkiw, R.: Simulation of Clothing with Folds and Wrinkles. *ACM SIGGRAPH/Eurographics Symposium on Computer Animation (SCA)* (2003) 28–36
14. Irving, G., Teran, J., Fedkiw, R.: Invertible finite elements for robust simulation of large deformation. In: *Proceedings of the ACM SIGGRAPH/Eurographics Symp. on Comput. Anim.* (2004) 131–140

15. Bonet, J., Wood, R.D.: Nonlinear continuum mechanics for finite element analysis. Cambridge University Press (1999)
16. Witkin, A., Baraff, D.: Physically Based Modeling: Principles and Practice. In: SIGGRAPH Course Notes. ACM Press/ACM SIGGRAPH (1997)
17. Wan, M., McNeely, W.A.: Quasi-static approach approximation for 6 degrees-of-freedom haptic rendering. In: Proceedings of IEEE Visualization 2003. (2003) 257–262